

Rayleigh-Taylor Instability Growth Rate Estimated Using WAM-IPE

Chun-Yen Huang¹, Tzu-Wei Fang², Arthur D. Richmond³, Timothy J. Fuller-Rowell¹¹ Cooperative Institute for Research in Environmental Sciences, University of Colorado Boulder, CO, USA² Space Weather Prediction Center, National Oceanic and Atmospheric Administration, CO, USA³ High Altitude Observatory, National Center for Atmospheric Research, CO, USA

Abstract: A simplified expression for Rayleigh-Taylor (R-T) growth rate is derived for direct estimation using the coupled Whole Atmosphere Model and Ionosphere Plasmasphere Electrodynamics model (WAM-IPE). The parameters of the expression are designed in apex coordinate (Richmond, 1995), which allows us to have more accurate and reasonable field line integrated conductivities and currents. The results demonstrate that the strong R-T growth rates are observed in uplifting ionospheric structure at the magnetic equator during post-sunset period. Diurnal and seasonal variations of the R-T growth rate are analyzed, revealing that the growth rates are most prevalent between 1800 LT and 2200 LT, with larger magnitudes observed at 284°E compared to 120°E and 0°E. Furthermore, equinox seasons exhibit more prominent growth rates compared to solstice seasons. These findings show the suitability of our proposed expression for calculating R-T instability growth rates using WAM-IPE. In our further investigation, we explored the relationship between the growth rate and S₄ scintillation and found that there is no direct correlation between the two. Moreover, the current estimation of growth rate using free run WAM-IPE does not correctly predict the occurrence of plasma bubble.

Rayleigh-Taylor Instability

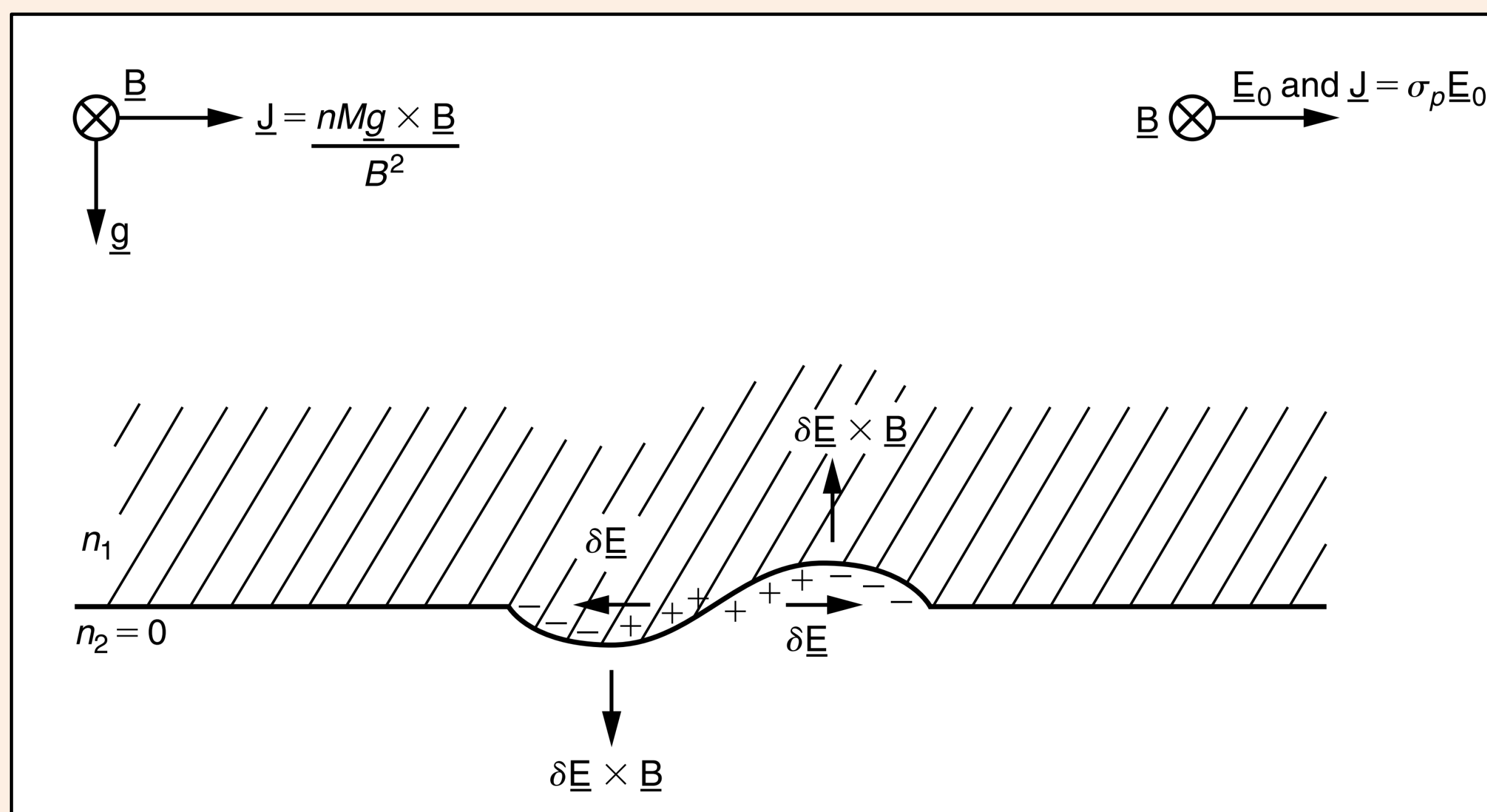


Figure 1. Schematic diagram of the plasma analog of the Rayleigh-Taylor instability in the equatorial region [Kelley, 2009].

- This phenomenon always occurs due to the significant reduction of the E-region in the post-sunset sector, leading to a large density gradient. The current is in the $g \times B$ direction, J_x will be large when n is large and small when n is small. Therefore, the charge will pile up on the edges of the small initial perturbation, resulting in perturbation electric field (δE) in the x direction and producing the plasma bubble.
- Another key factor induced the occurrence of plasma bubble is the pre-reversal enhancement (PRE) in the post-sunset sector, which pushes the ionosphere to the high altitude and makes it more unstable.

Expression for Rayleigh-Taylor Instability in Apex Coordinate

$$\frac{\partial n}{\partial t} + \nabla \cdot \left(\frac{n}{B^2} \vec{E} \times \vec{B} \right) + \nabla \cdot (n \vec{v}_i) = q - l$$

$$\Rightarrow \frac{\partial \eta'}{\partial t} + \frac{v'_{e1}}{\cos \lambda_m} \frac{\partial \eta_0}{\partial x} - \frac{v'_{e2}}{\cos \lambda_m} \frac{\partial \eta_0}{\partial y} = 0$$

$$\Rightarrow \frac{\partial \eta'}{\partial t} - \frac{(\Sigma_x^E E_x + K_x^{DF} - \Sigma_c^E E_y)}{\Sigma_x B_{e3} \cos^2 \lambda_m \eta} \frac{\partial \eta}{\partial y} \eta' = 0$$

$$\frac{1}{\eta_0} \frac{\partial \eta_0}{\partial y} \approx \frac{1}{K_x^{GF}} \frac{\partial K_x^{GF}}{\partial y} \Rightarrow \gamma = \frac{(\Sigma_x^E E_x + K_x^{DF} - \Sigma_c^E E_y)}{K_x^{GF} \Sigma_x B_{e3} \cos^2 \lambda_m} \frac{\partial K_x^{GF}}{\partial y}$$

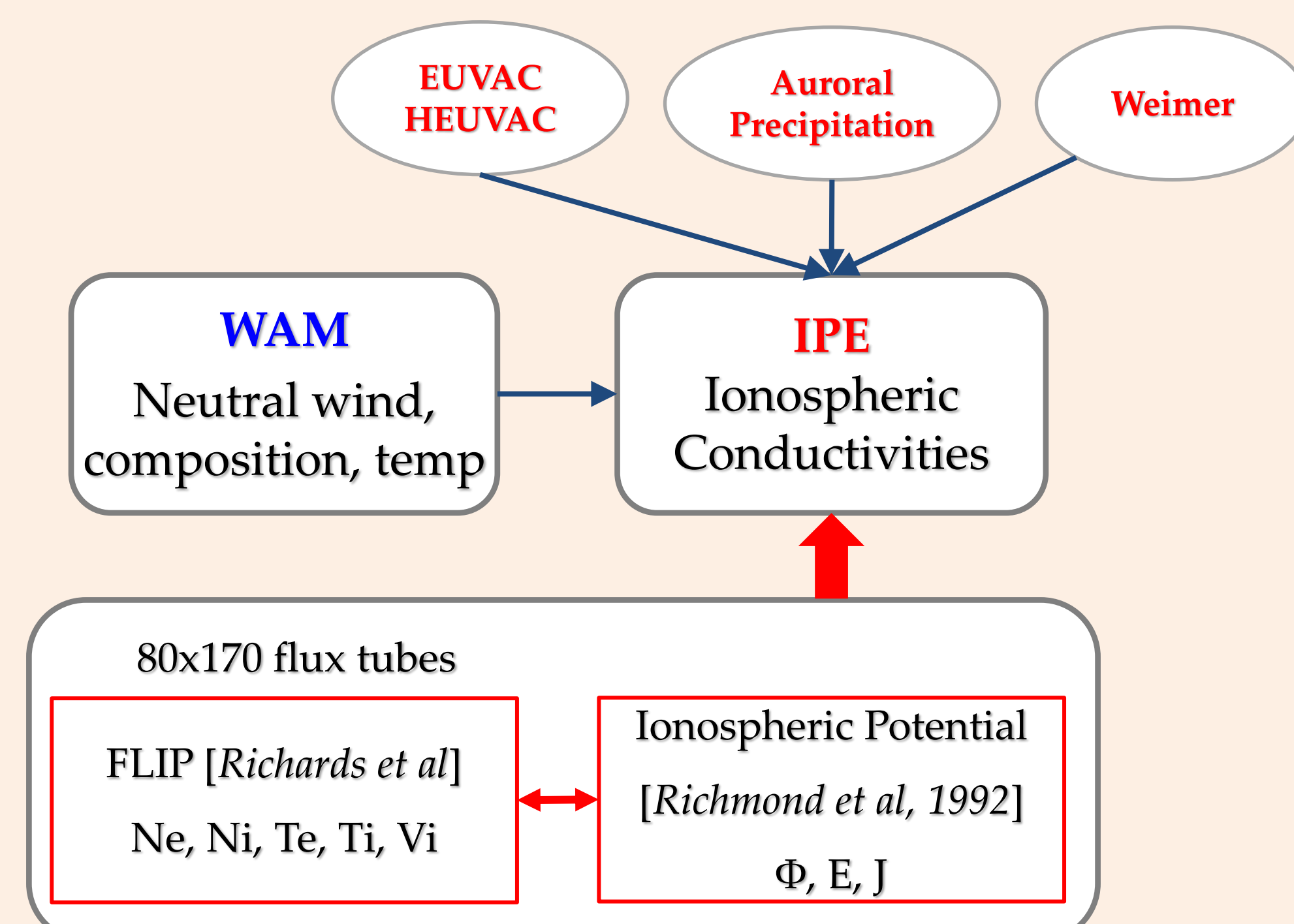
$$K_x^{DF} = B_{e3} \cos \lambda_m \int_{S(150)}^{N(150)} \left[\frac{\sigma_p d_1^2}{D} u_{e2} + \left(\sigma_H - \frac{\sigma_p d_1 \cdot d_2}{D} \right) u_{e1} + \frac{nm_1 e_2 \cdot g}{B_{e3} B} \right] ds$$

$$K_x^{GF} = \cos \lambda_m \int_{S(150)}^{N(150)} \frac{n_0 m_1 e_2 \cdot g}{B} ds$$

- The simplified function for calculating the R-T growth rate is similar with the function derived by Sultan (1996), but the parameters have been projected onto the apex coordinate. We assume that the ionosphere is stable, and the recombination effects are small above 300 km [Bittencourt and Abdu 1981]. Thus, we didn't take the recombination rate into account.
- The field line integrated parameters can be output by WAM-IPE, allowing for direct calculating the R-T growth rate. The lower boundary for Σ_x is 90 km, for other parameters is 150 km.

Whole Atmosphere Model (WAM)

- Extended Global Forecast System (GFS) upper boundary from 64 km to 600 km
- Resolution 4°×4° in latitude-longitude
- Free or forecast runs
- Horizontal & vertical mixing
- Radiative heating (EUV & UV) and cooling
- Ion drag & Joule heating
- Major species composition
- Non-orographic and orographic gravity waves
- TIROS Auroral & NASA/SDO EUV



Ionosphere Plasmasphere Electrodynamics (IPE) Model

- Built upon the field line interhemispheric plasma (FLIP) model.
- The spatial resolution varies between approximately 1.26° and 0.24° in magnetic latitude beyond and within ±30°, while remaining consistent at 4.5° in magnetic longitude.
- International Geomagnetic Reference Field (IGRF) and Apex coordinate system [Richmond, 1995] are applied.
- Conductivities and dynamo currents are integrated along the field lines for solving the Electrodynamics.

Acknowledgment: The authors gratefully acknowledge support from the National Science Foundation's Space Weather with Quantification of Uncertainties program under grant number AGS 2028032

Longitudinal Distribution of R-T Growth Rate

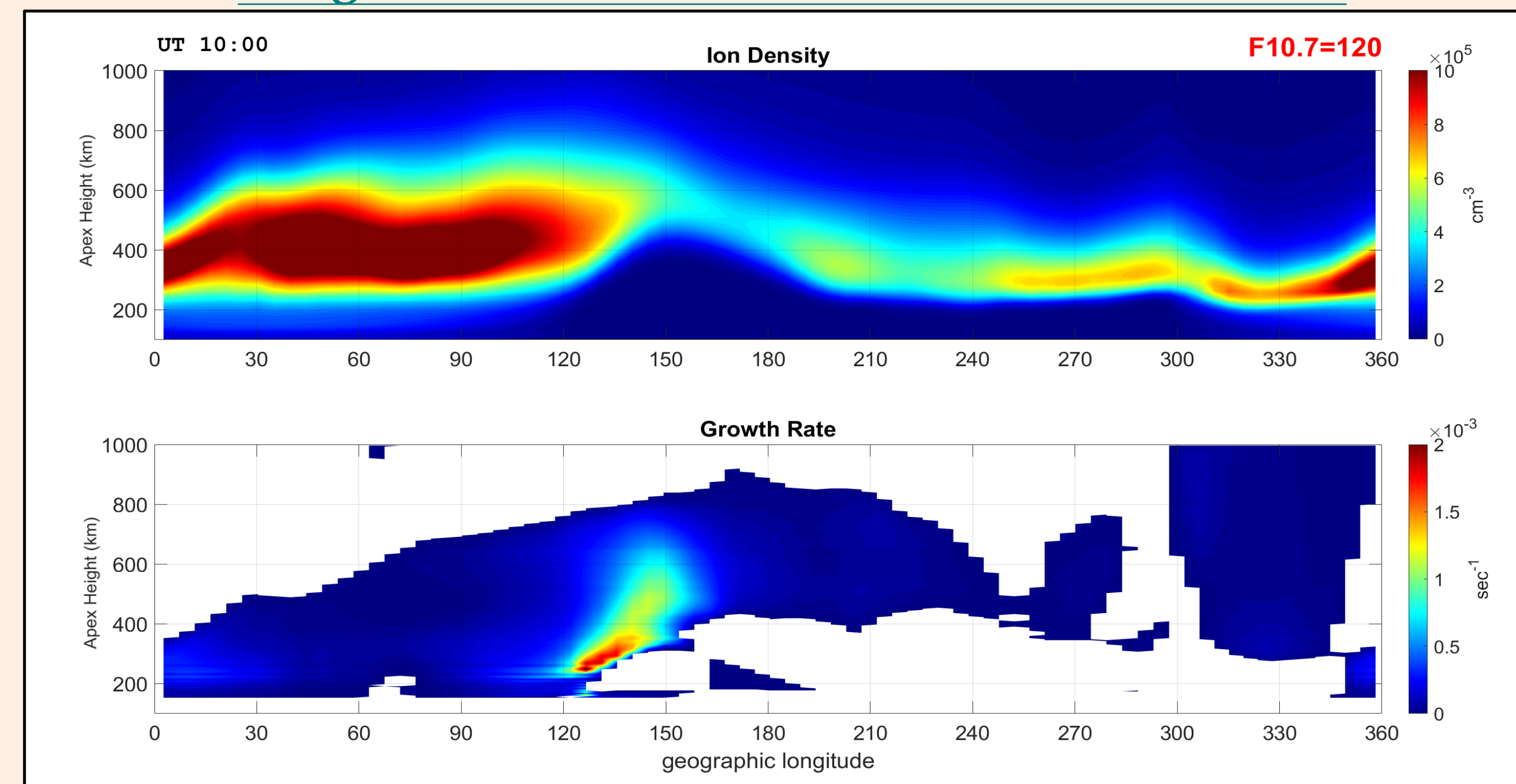


Figure 2. WAM-IPE ion density (top) and the R-T growth rate at the magnetic equator on March equinox. The model is driven by F10.7 = 120 and Kp = 1.

- Significant growth rates can be observed just below the F₂ peak in the tilt structure, specifically between longitudes 120°E and 150°E. This simulation aligns with previous studies indicating that the vertical drift induces instability in the ionosphere.
- The result shows that the new expression combined with WAM-IPE has the capability to estimate a reasonable R-T growth rate, and the magnitudes are comparable with Huba (2022).

Diurnal Variations at Different Longitude

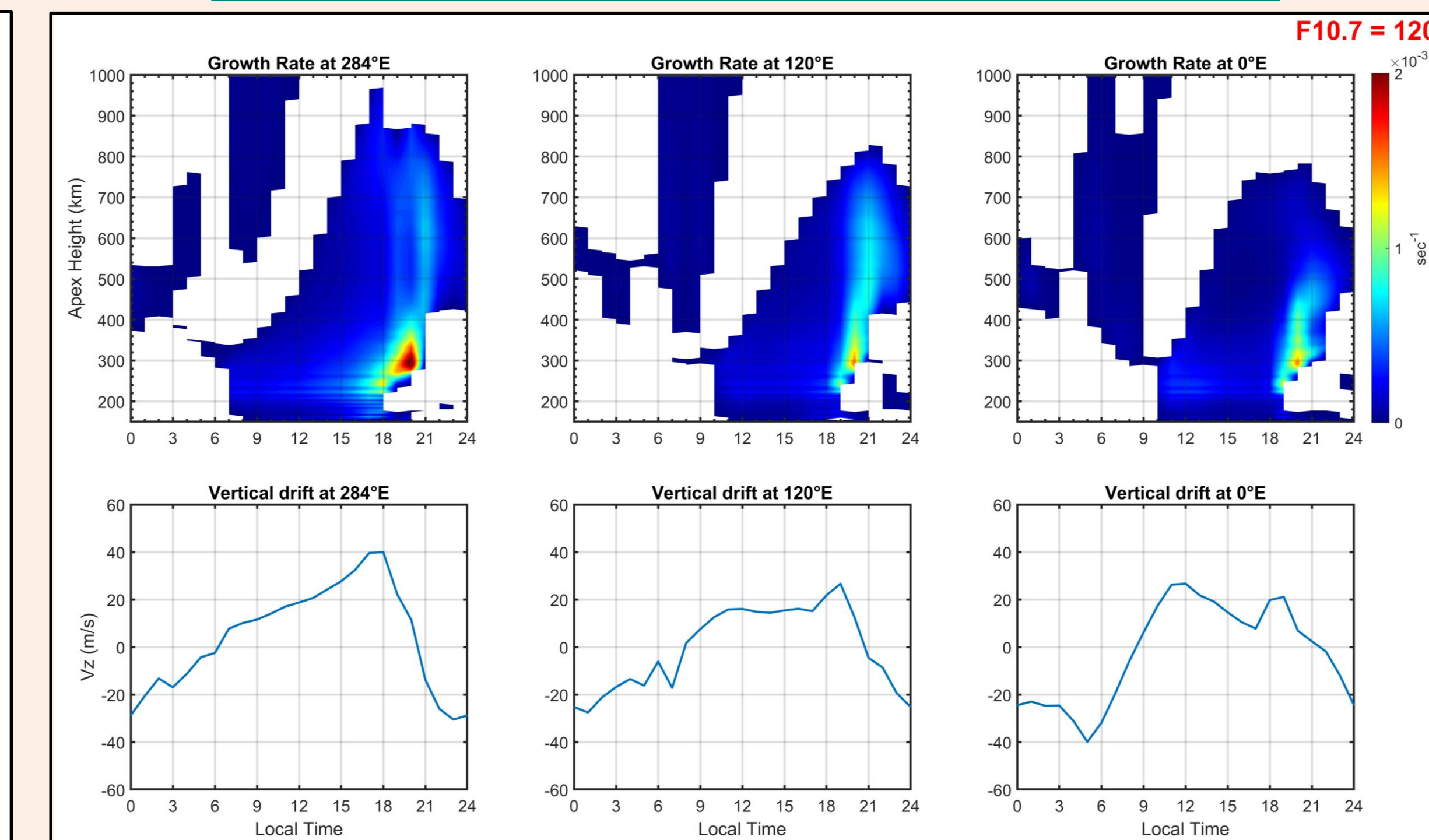


Figure 3. Diurnal variations of the R-T growth rate (top panel) and vertical drift at 300 km (bottom panel) at magnetic equator different geographic longitude in March. From left to right panel is at 284°E, 120°E, and 0°E, respectively. The model applies fixed F10.7 of 120 and Kp of 1.

- Large magnitude of growth rate can be observed at around 1800 LT ~ 2200 LT, which is consistent with previous studies [e.g., Fejer et al., 1999; Rajesh et al., 2017].
- The growth rate at a longitude of 284°E is greater than that of other longitudes and demonstrates a correlation with PRE vertical drift at all longitudes.
- The growth rate at 284°E is larger than other two, which may result from the differences of the declination angle.

Seasonal Variations

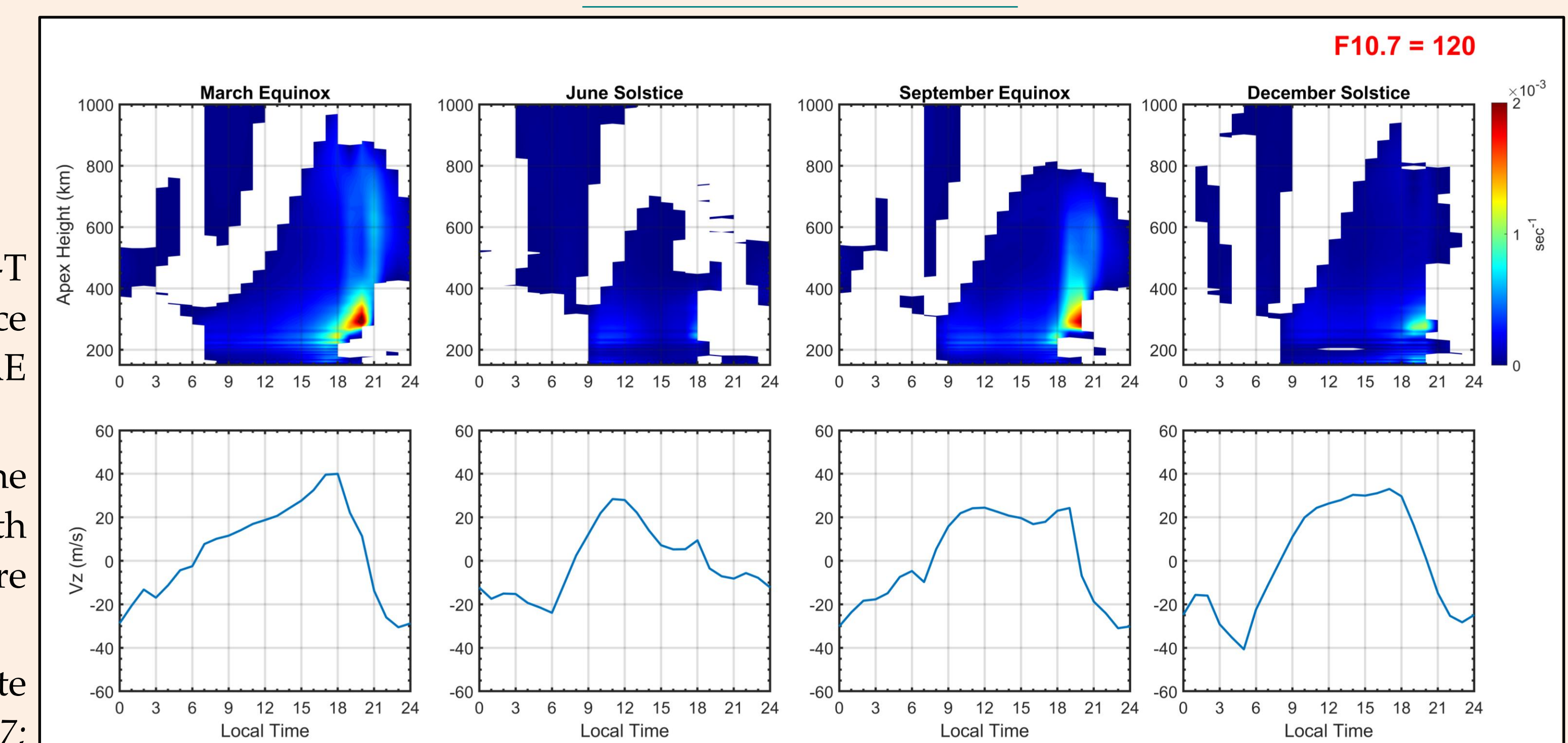


Figure 4. Seasonal variation of R-T growth rate (top) and vertical drift (bottom) at 284°E at magnetic equator under F10.7 of 120 and Kp of 1 (right).

- In equinox seasons, the magnitude of the R-T growth rate is larger compared to the solstice seasons, and it's attributed to the stronger PRE vertical drift.
- In December solstice, the vertical drifts in the daytime and evening are strong, but the growth rate is faint, which might be due to the obscure PRE feature.
- The overall seasonal variation agree with satellite observations [e.g., Su et al., 2006; Liu et al., 2017; Huang et al., 2022].

R-T Growth Rate vs. Observations

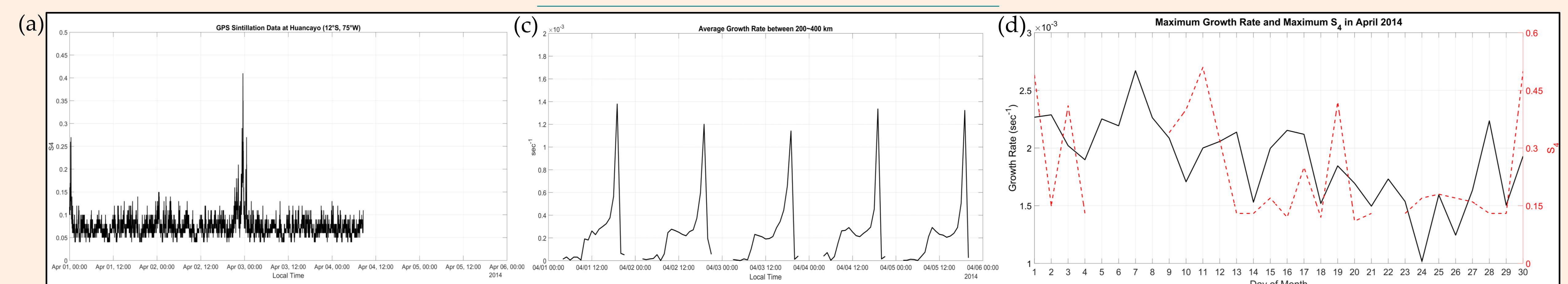


Figure 5. (a) maximum values of 32 GPS scintillations at Huancayo (12°S, 75°W), (b) airglow image in the 630.0 nm at Jicamarca (12°S, 76°W), (c) average growth rate between 200-400 km at around Jicamarca region, and (d) comparison of maximum scintillation from 1900 to 0200 LT and maximum growth rate from 1900 to 2200 LT in April 2014. (S₄: <http://lisn.igpp.gov.pe/>, all-sky imager: <http://sirius.bu.edu/>)

- In general, airglow depletions are associate with plasma depletions, where the associated plasma bubbles result in remarkable range spread-F layers, which further cause intense amplitude scintillations of GNSS signals.
- The growth rate, which represents how fast the perturbations grow, cannot be directly used to represent plasma bubbles. Thus, we picked the maximum value to compare with S₄ scintillation.
- The great scintillation agrees well with the airglow depletions on 02 April-03 April, but the growth rates do not match the observations and incorrectly predict the occurrences of plasma bubble in April 2014.

Summary and Future Work

- The larger growth rates mainly appear at uplifting ionospheric structure in the post-sunset period, and strongly associate with PRE vertical drift. The diurnal variation, the seasonal variation, and the magnitude of growth rate in show agreements with previous study. These depict our expression for calculating R-T instability growth rate using WAM-IPE is appropriate.
- The growth rate shows obvious day-to-day variation, indicating the sensitivity of the simulation to vary with the diurnal ionospheric structure.
- The current use of free run WAM-IPE for estimating the R-T growth rate is not sufficient for predicting the occurrence of plasma bubbles. As the result, we are actively working on incorporating additional factors to enhance our predictions.